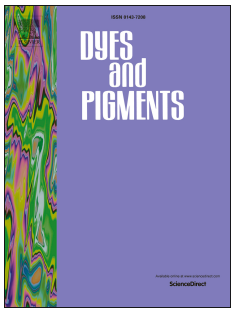

Dual-function fluorescent probe with red emission for sensing viscosity and OCl^- and its applications in bioimaging

Fanyong Yan, Xiaodong Sun, Yingxia Jiang, Ruijie Wang, Yuyang Zhang, Yali Cui

PII: S0143-7208(20)30779-8

DOI: https://doi.org/10.1016/j.dyepig.2020.108531

Reference: DYPI 108531

To appear in: *Dyes and Pigments*

Received Date: 28 March 2020

Revised Date: 8 May 2020

Accepted Date: 8 May 2020

Please cite this article as: Yan F, Sun X, Jiang Y, Wang R, Zhang Y, Cui Y, Dual-function fluorescent probe with red emission for sensing viscosity and OCl^- and its applications in bioimaging, *Dyes and Pigments* (2020), doi: https://doi.org/10.1016/j.dyepig.2020.108531.

Fanyong Yan and Xiaodong Sun: Conceptualization, Methodology. Xiaodong Sun, Yingxia Jiang, Ruijie Wang and Yali Cui: Experiments, Methodology, Software. Xiaodong Sun, Yingxia Jiang, Yuyang Zhang: Writing-Original draft preparation. Fanyong Yan, Yali Cui: Supervision, Validation, Writing-Reviewing and Editing.

Dual-function fluorescent probe with red emission for sensing viscosity and OCl^- and its applications in bioimaging

Fanyong Yan [§ a] *, Xiaodong Sun [§ a], Yingxia Jiang [a], Ruijie Wang [a], Yuyang Zhang [a], Yali Cui [b]

a State Key Laboratory of Separation Membranes and Membrane Processes/National Center for International Joint Research on Separation Membranes, School of Chemistry and Chemical Engineering, Tianjin Polytechnic University, Tianjin 300387, P.R. China

b Department of Nuclear Medicine, Harbin Medical University Cancer Hospital, Harbin, Heilongjiang, 150081, P.R. China

§ Those authors contribute equally to the article

***Corresponding author. Tel: +86 22 83955766. E-mail addresses: yanfanyong@tiangong.edu.cn (Fanyong Yan).**

Abstract

The microenvironment in biological systems is associated with pathological of organisms. In this work, HBTC, a red-emitting probe with abilities of responding to OCl^- and environmental viscosity was designed and synthesized to preliminary apply in cell imaging. HBTC showed weak fluorescence in the dissolved state due to intramolecular rotation, and it showed about 620 nm red light emission when molecules are restricted. Through red-to-turquoise ratiometric fluorescence signal, HBTC showed the capacity to selective detecte OCl^-, and the LOD was calculated to be 0.141 μM in OCl^- concentration range of 2 – 20 μM. Finally, HBTC was used for preliminary cell fluorescence imaging. It is expected that HBTC will be used to study the diseases related between OCl^- concentration and viscosity in cells.

Keywords: Fluorescent probe; OCl^-; Viscosity; Cell imaging

1 Introduction

Hypochlorous acid (HOCl)/hypochlorite (OCl^-) as an essential biological active oxygen (ROS) plays an important role in the body, relating to many physiological processes such as cell differentiation, conduction, migration, and immune system.[1-5] OCl^- is produced in the organism by H_2O_2 and Cl^- under the catalysis of myeloperoxidase (MPO), thereby exerting its biological function.[3, 6, 7] OCl^- can play protective function about health in the organism, but abnormal concentrations of OCl^- can cause diseases such as arthritis, rheumatoid disease, tissue damage, lung injury, kidney disease, cardiovascular disease, neuronal degeneration and even cancer.[8, 9] Therefore, the detection of OCl^- in biological systems is particularly important. On the other hand, the change in intracellular viscosity is also an important parameter. The interaction between biomolecules and chemical in cell is concerned with cellular viscosity, therefore, many diseases and cellular malfunctions are related to it.[10, 11] Apoptosis of the cell is also accompanied by changes in intracellular viscosity.[12, 13] The cellular apoptosis caused by disease about excess OCl^- may be a condition linked to both parameters, thus it is of great significance that develops methods capable of detecting both indexes simultaneously in cell. Traditional detection methods such as mass spectrometry, ion chromatography, electrical analysis, potentiometer, mass spectrometry, and

nuclear magnetic methods,[14] these methods are difficult to apply to biological systems, and it is almost impossible to detect changes in viscosity and OCl^- at the same time. Therefore, it is necessary to find a new detection method.

Fluorescence analysis is an emerging detection method. As a powerful analysis tool, it has the advantages of flexible application, sensitive signals, easy operation, and economical practicality.[15, 16] In addition, the most important feature compared to traditional detection methods is that it can enter the organism to perform functions.[17, 18] Due to its own fluorescence emission characteristics, biological tissues have strong fluorescence interference in the blue to green band during fluorescence observation.[19-21] This background light has a greater impact on fluorescent probes in this wavelength range, which is not conducive the process of fluorescence analysis.[22-24] Another disadvantage of short wavelength light is the damage of high energy light to biological systems.[25, 26] The feasible solution is the fluorescent probe with a large Stokes shift, thereby reducing the effect of background light and organism damage.[27] In addition, another advantage of long-wavelength emission is its strong penetrability, which makes it possible to image deeper tissues and noninvasive in vivo imaging.[28, 29] Therefore, fluorescent probes with long-wavelength emission have attracted much attention due to their unique advantages in imaging.

The probe achieves two functions in one molecule and can easily analyze the relationship between related functions. Qiu et al. synthesized a probe that can sequentially responded Co^{2+}, Hg^{2+}, and Cu^{2+}, which is due to the affinity of phenolic hydroxyl and imine for divalent cations.[30] Based on the metabolic process of cysteine (Cys), Yue et al. synthesized a probe with capable of responding to Cys and SO_2 simultaneously and successfully applied it to observe the metabolic process of Cys in zebrafish.[31] Li et al. synthesized a NIR probe that responds to both viscosity and hydroxyl radical, which successfully associated it with Ferroptosis.[32] Long-wavelength emission probes that respond to viscosity and OCl^- are rarely reported. In order to study the intrinsic relationship between them, it is necessary to develop a dual-functional probe with the abilities. For achieving this purpose, we obtained HBTC by prolonging the conjugated structure of HBT, and it showed AIE properties and OCl^- response capabilities in cells imaging.

2 Experimental

2.1 Materials and instruments

Trifluoroacetic Acid (TFA), salicylaldehyde, and acetoacetic ester was purchased from Tianjin Kemiou Chemical Reagent Co., LTD. Analytical grade 2-aminobenzenethiol was purchased from Aladdin Reagent Co., LTD. Hexamethylenetetramine (HMTA) was purchased from Tianjin Guangfu Technology Development Co., LTD. Other solvents and test agents were purchased from Tianjin Fengchuan chemical reagent technology Co., LTD. All reagents and solvents were used directly without further purification. Thin layer chromatography (TLC) and column chromatography (200-300 mesh silica gel) were purchased from Qingdao Ocean Chemical Co., LTD. Distilled water was used during all test.

Fluorescent spectra were measured by F-380 fluorescence spectrophotometer. FT-IR spectra were obtained by TENSOR37 FT-IR (KBr disks). The pH values were carried out on a Mettler Toledo pH meter. NMR spectra were measured by Bruker Advance III HD 400MHz spectrometer. UV–vis spectra were obtained by Purkinje General TU-1901 UV–vis spectrometer. Bioimaging was obtained through Leica SP5 confocal microscopy. HRMS was obtained by Bruker micro TOF-QII instrument.

2.2 Synthesis of probe HBTC

3-acetyl-2H-chromen-2-one (3-acetylcoumarin). Salicylaldehyde (2 mL, 19.16 mmol) and ethyl acetoacetate (3.63 mL, 28.74 mmol, 1.5 eq), respectively was added to a three-necked flask with 30 mL of ethanol, two drops of piperidine were added dropwise, heated to reflux, and monitored by TLC. After the starting point of the system disappeared, the solution was concentrated by rotary evaporation and recrystallized with ethanol to obtain 2.82 g (y% 78.21%) of white crystals.

3- (3- (3- (benzo [d] thiazol-2-yl) -2-hydroxyphenyl) acryloyl) -2H-chromen-2-one (HBTC). The synthesis of HBT-CHO accords the pervious reporter.[33] HBT-CHO (0.2 g, 0.78 mmol) and 3-acetylcoumarin (0.44 g, 2.35 mmol, 3 eq) were added to 30 mL of ethanol, two drops of piperidine were added dropwise, and the reaction was monitored by TLC with reflux. Until the system no longer changes, the reaction solution was poured into cold water, filter, dry, and purify by column chromatography (PE / EA = 10/1) to obtain a yellow solid (0.16 g, y% = 45.00%). ^{1}H NMR (400

MHz, $CDCl_3$) δ 13.52 (s, 1H), 8.59 (s, 1H), 8.31 (s, 1H), 8.14 (s, 1H), 8.01 (d, *J* = 6.5 Hz, 1H), 7.92 (d, *J* = 8.0 Hz, 1H), 7.81 – 7.73 (m, 2H), 7.67 (dd, *J* = 14.3, 7.7 Hz, 2H), 7.53 (t, *J* = 7.6 Hz, 1H), 7.49 – 7.36 (m, 2H), 7.35 (d, *J* = 7.3 Hz, 1H), 7.01 (s, 1H). ^{13}C NMR (101 MHz, DMSO) δ 187.63 (s), 163.65 (s), 158.56 (d, J = 7.8 Hz), 154.42 (s), 151.38 (s), 146.37 (s), 144.41 (s), 134.82 (s), 134.03 (s), 132.28 (s), 130.33 (s), 129.85 (s), 126.55 (s), 126.32 (s), 125.98 (s), 125.21 (s), 124.96 (s), 123.08 (s), 122.31 (s), 122.10 (s), 119.28 (s), 118.53 (s), 117.81 (s), 116.26 (s). HRMS (ESI-, m/z): Calcd for $[M-H^+]^-$ 424.0649; found, 424.0657.

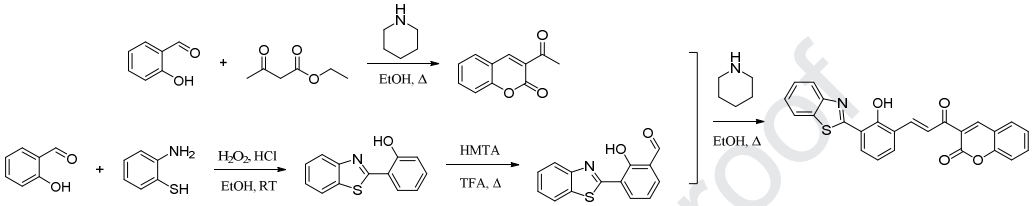

Scheme 1. The synthetic route of HBTC.

2.3 Optical measurement

HBTC was dissolve in DMSO to prepare a 0.2 mM mother liquor. Analytes include NaF, NaCl, NaBr, NaI, NaH_2PO_4, Na_2HPO_4, $NaNO_2$, Na_2SO_3, Na_2SO_4, $Na_2S_2O_3$, $Na_2S_2O_8$, NaS, $NaHSO_3$, NaAc, $KMnO_4$, NaOCl, H_2O_2, t-BuOOH, ·OH (1 mM Fe^{2+} with 100 μM H_2O_2), $ONOO^-$, $O_2^{\cdot-}$ (300 μM xanthine with 2.5 U/mL xanthine oxidase), GSH, Hcy, and Cys.[34, 35] The inorganic salts were prepared into a mother solution of 0.2 mM by secondary distilled water. The test of AIE properties was carried out in different ratios of MeOH/Tris solution system.[36] The volume ratio of MeOH was 0/10 – 10/0, and the final HBTC concentration was 10 μM. Viscosity test was prepared according to glycerol/MeOH 2/8 – 10/0, and the final HBTC concentration was 20 μM.[37] The rest of the spectral tests were performed in MeOH/Tris (20/80, v/v, 0.05 mM, pH 7.4) unless otherwise specified. All spectral tests were performed in a 1 × 1 × 3.5 cm quartz cuvette.

2.4 Cell imaging

According a usual program, MDA-MB-231 cells were cultured in a 5% CO_2 saturated water incubator containing 10% FBS with Penicillin and Streptomycin at 37 °C. HBTC (1 mM, 10 μL) was added to a 35 mm glass-bottomed petri dish with MDA-MB-231 cells for another 1 h at 37 °C, then washed by PBS twice. For evaluating the functions of HBTC, the cells were divided into three groups: blank, Taxol (1 mM, 10 μL), and OCl^- (1 mM, 10 μL) were added to the medium for another 30 min, respectively. After washes in PBS twice, fluorescence images were recorded by a

fluorescence confocal microscope.

3 Results and discuss

3.1 Fluorescent properties of HBTC

The fluorescent properties of HBTC were first tested. In solid state, HBTC is a yellow powder and emits red fluorescence under ultraviolet light. As shown in Fig. 1a, the emission spectrum shows a narrow band at 620 nm, the peak of its excitation spectrum at 406 nm, and the Stokes shift value reaches about 214 nm. Subsequently, the fluorescence spectra in different MeOH/Tris solvent systems was recorded. As the proportion of organic solvents continues to decrease, the red fluorescence of HBTC continues to increase by about 13 times, and the most obvious changes after the 1:1 solvent system. At the same time, at the edge of the fluorescence spectrum, the Rayleigh peak resulted from excitation spectrum increases with water content, which shows HBTC precipitates and agglomerates in water. Prior to this, the solution showed little red fluorescence and a slight blue fluorescence at 455 nm. These phenomena indicate that HBTC has AIE property,[38, 39] and the enhanced red fluorescence is consistent with the phenomenon of AIE (Fig. 1b). It is the general understanding about AIE phenomenon that the freely rotating single bond of fluorescent molecules is limited by the environment, producing enhancement in fluorescence signal. There are several freely rotating single bonds in HBTC molecules, demonstrating the potentiality of the AIE properties of the HBTC molecule.

The viscosity of solution is a condition to effectively limit the free-rotating single bond, thereby achieving AIE process of HBTC. MeOH/glycerol solution of different ratios was used as a tool to change the viscosity of the solution system. As shown in Fig. 1c, the fluorescence peaks at 455 nm and 620 nm enhanced as the proportion of glycerol increases, and these two peaks finally make the color of solution gradually become pale white fluorescence with color coordinates (0.31, 0.25) (Fig. S5) that is close to white emission. It is strange that the blue fluorescence changes with viscosity and even more susceptible to viscosity (Fig. 1c). The possible cause of the phenomenon is multiple freely rotatable single bonds in the structure of HBTC, and their sensitivity to viscosity is different, which leads to HBTC showing two AIE fluorescence peaks at the same time. It can be speculated that the single bond connecting the coumarin molecule is more susceptible to the influence of

viscosity, so the blue fluorescence may be due to the emission from this part. As shown in Fig. 1d, The Förster-Hoffmann equation was fitted to the peak of blue fluorescence and viscosity (η, 4.83 – 945 cP, Table S1) to obtain the curve: $\log F_{455} = 0.383\log\eta + 1.704$ ($R^2 = 0.9762$).[32] In summary, HBTC has a large Stokes shift, obvious AIE properties, multiple flexible single bonds, and viscosity-related fluorescence properties.

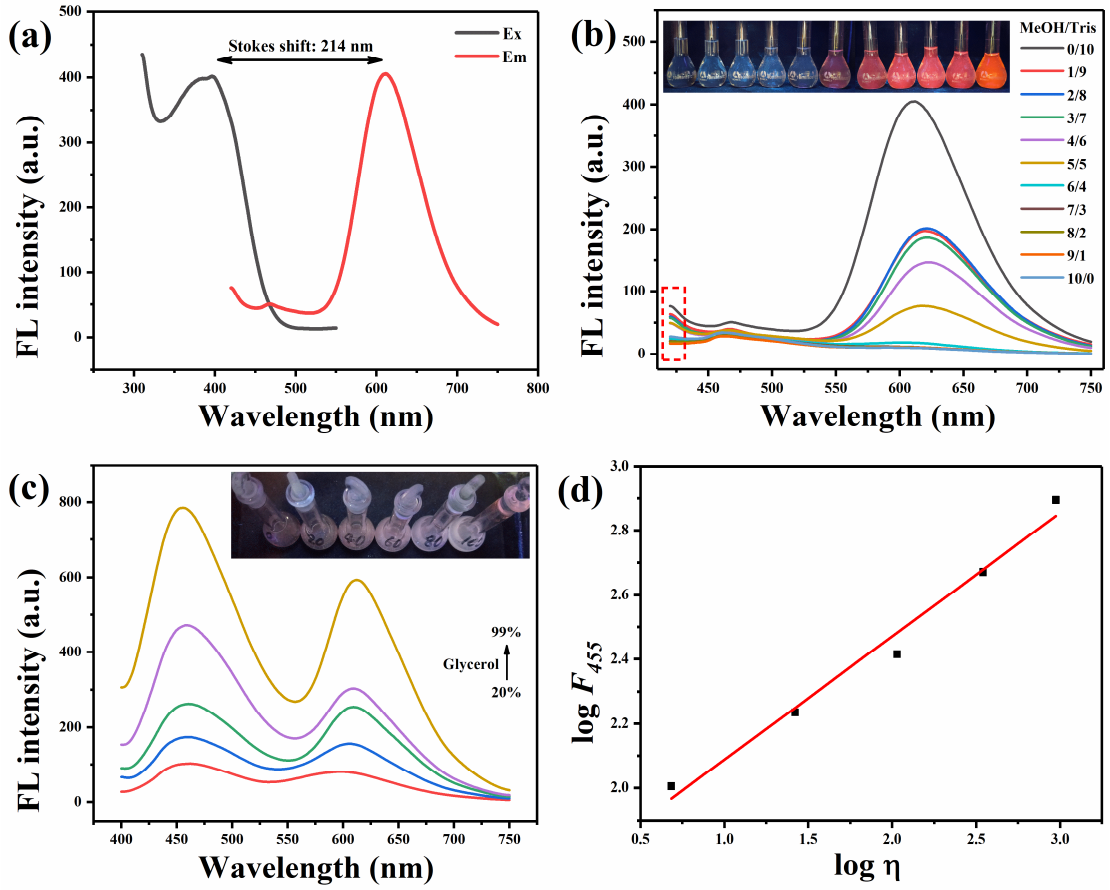

Fig. 1. Fluorescence properties of HBTC. (a) Optimal excitation and emission wavelengths of HBTC; (b) Changes in fluorescence spectrum caused by different ratios of MeOH/Tris (insert: physical photos); (c) Changes in fluorescence spectrum caused by viscosity (insert: physical photos); (d) Förster-Hoffmann equation fitted by viscosity and fluorescence.

3.1 The detection of HBTC to OCl^-

For evaluating specificity of HBTC, the detection of different anions and active species was carried out. As shown in Fig. 2a, among the 22 species tested, OCl^- showed obvious fluorescence changes, and the fluorescence color of the solution changed from red to turquoise. H_2O_2 and ·OH showed a slight fluorescence change, and the remaining species were almost does not affect the color change of the solution. From the selective experiments, it can be indicated that only OCl^- can respond to HBTC and get obvious fluorescence changes among 22 species. Subsequent interference

experiments also obtained the same conclusion. As shown in Fig. 2b, the response of OCl^- to HBTC in the presence of other species has little effect on the fluorescence intensity at 620 nm and 506 nm. This reveals strong anti-interference ability. The fluorescence at 620 nm decreased and the fluorescence at 506 nm increased as the concentration of OCl^- continued to increase, and a significant change in fluorescence color was observed (Fig. 2c). The natural logarithm of the fluorescence ratio I_{620}/I_{506} shows good linearity in a concentration change of 2 – 20 μM, fitting curve: $\ln(I_{620}/I_{506}) = -0.242[OCl^-] + 2.851$, $R^2 = 0.9827$, and the corresponding LOD for OCl^- is calculated to be 0.141 μM (3σ/k, Fig. 2d).

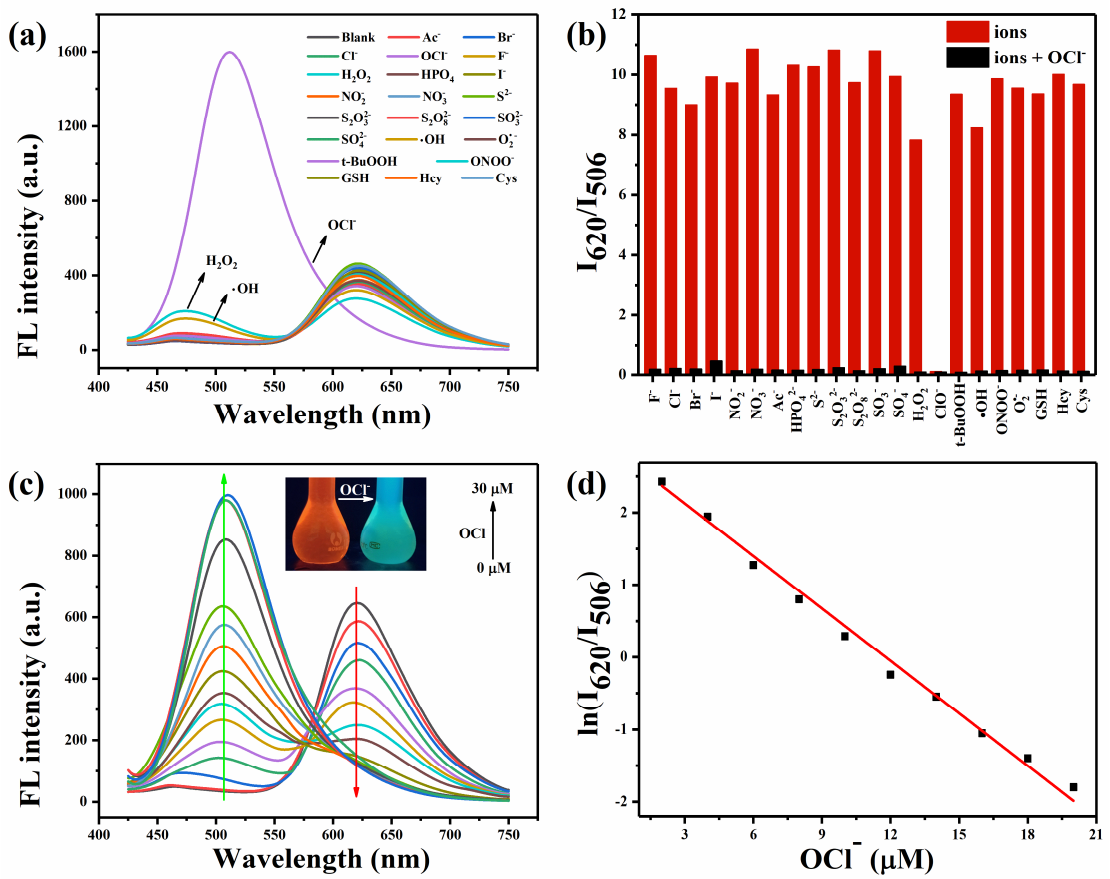

Fig. 2. The detection of HBTC to OCl^-. (a) The fluorescent spectra of HBTC to different species; (b) I_{620}/I_{506} value of HBTC in the presence of OCl^- with the addition of competitive species; (c) Fluorescent spectra of HBTC in the presence of different concentrations OCl^- (insert: photos of before and after OCl^- addition); (d) Fitting curve of $\ln(I_{620}/I_{506})$ value versus OCl^- concentration of (2 − 30 μM).

The details of detecting OCl^- need further explanation. As shown in Fig. S6a, HBTC showed a significant fluorescence change within a few seconds after OCl^- was added. The ratio fluorescence reached the endpoint of detection about 2 min, and then remained stable. The effect of pH on the detection is shown in Fig. S6b. In the range of pH from 6 to 9, HBTC has a convictive detection

effect on OCl^-. Fluorescence of HBTC changes under partial acid or alkaline conditions, which indicates that the solution conditions can affect the fluorescence of HBTC. The structure of HBTC contains a phenolic hydroxyl group, indicating that it is easily affected by alkaline environment. In order to prove that alkaline conditions and OCl^- have different effects on HBTC, three different solution conditions were prepared as follows: EtOH/Tris (1/1, v/v; pH 7.4), EtOH/Tris (1/1, v/v; pH 11), and EtOH/Tris (1/1, v/v; pH 11) containing OCl^-. As shown in Fig. S6c, HBTC has two characteristic absorption peaks at 400 nM and 470 nM under neutral conditions. At alkaline conditions, the absorption peak at 400 nM disappeared, but the absorption peak at 470 nM increased, and the solution was brown under sunlight. It can be found in the fluorescence spectrum that the color of the fluorescence changed to blue at pH = 11. However, the color of the fluorescence is slightly different from that under alkaline conditions, and the fluorescent peak appears around 470 nm. (Fig. S6d). Changes in absorbance and fluorescence indicate that OH^- and OCl^- have different effects on HBTC.

3.3 Proposed explanation of detection mechanism

In previous experiments, it can be revealed that both alkaline conditions and OCl^- can make HBTC fluorescence change, and the fluorescent peaks difference is about 30 nm. Therefore, the structural changes of HBTC under different conditions need to be further proved. The fluorescence change of HBTC under alkaline conditions can be reasonably inferred: the deprotonation effect of the phenolic hydroxyl group can cause the ESIPT process to occur, which ultimately brings a change in color. The mechanism of OCl^- response needs to be further discussed. In the reference, the reaction mechanism was speculated that phenol structure is oxidized to quinone structure by OCl^-.[40, 41] Based on this, a similar mechanism is guessed and verified by ^1H NMR to explain the experiment. It can be found in Fig. 3 that the proton peak on the phenolic hydroxyl group disappears after the response of HBTC to OCl^-, and the proton peak (b) of the hydroxyl counterpoint on the benzene ring disappears. In addition, the completion of the reaction caused the movement and deformation of most of the proton peaks, such as the movement of the proton peak (c) on the conjugated double bond. HRMS also proved this process. As shown in Fig. S7, ion peak emerged at m/z 440.0613 (Calcd for $C_{25}H_{14}NO_5S^+$ 440.0587), representing the formation of p-benzoquinone derivatives. Therefore, the detection mechanism was preliminarily considered through ^1H NMR and

HRMS.

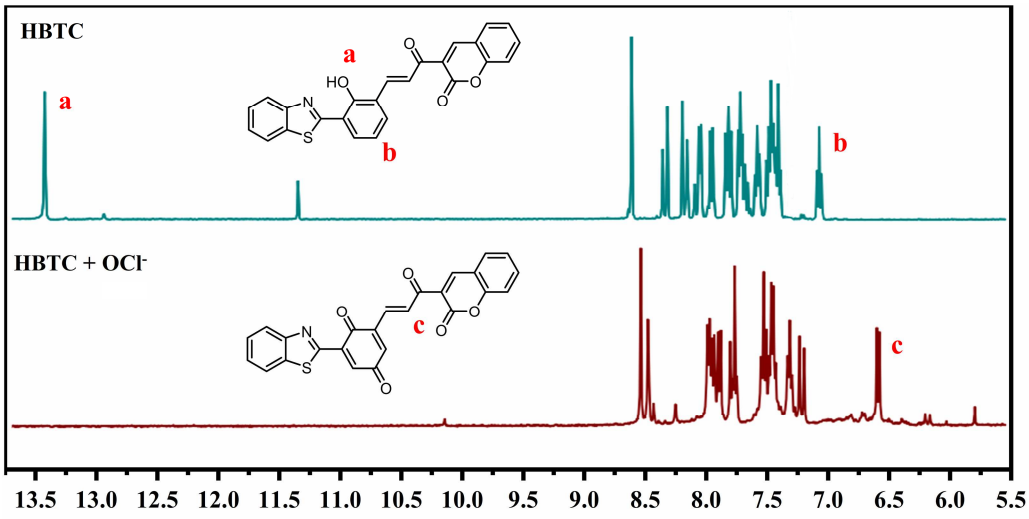

Fig. 3. Changes in ^{1}H NMR peaks of HBTC and HBTC + OCl$^-$ (d-DMSO).

In summary, three types of HBTC response are reasonably assumed: the redox process with OCl$^-$, the ESIPT effect under alkaline conditions, and the viscosity-dependent internal rotation restricted process, which cause changes of the fluorescence (Scheme 2).

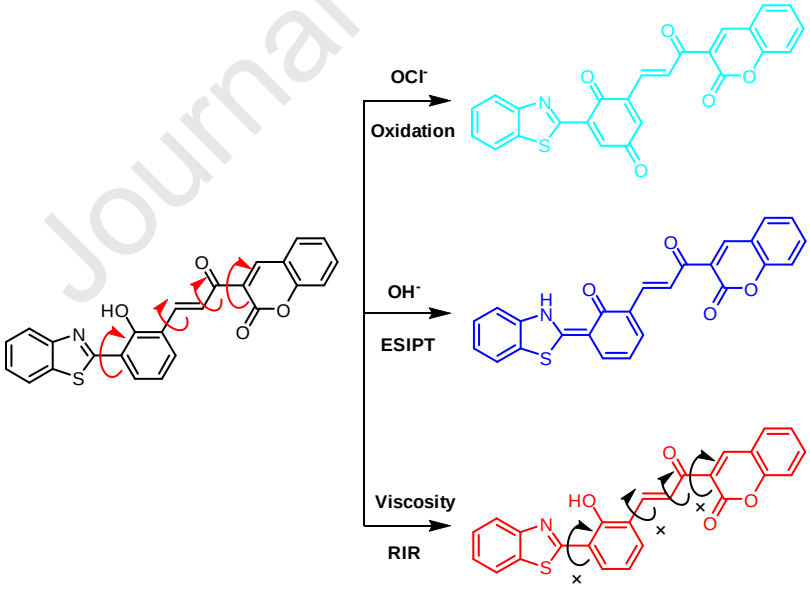

Scheme 1. Three variations of HBTC in different conditions.

4 Application of HBTC in cell imaging

Cell apoptosis will lead to morphological changes and abnormal intracellular indicators, where changes in viscosity have been reported in many literatures.[12, 13] In order to show whether HBTC

can change color with the viscosity change during apoptosis, co-culture staining of HBTC and breast cancer cells was performed. As shown in Fig. 5, the cancer cells respectively showed fluorescent signal in the red channel and the blue channel in the case of HBTC alone. After adding Taxol to promote apoptosis, it is disappointing that the fluorescence signal enhancement is not obvious. Probable cause is that HBTC is not sensitive to changes in viscosity caused by apoptosis, and it can also be seen from Fig. 1. Another possible cause is that the watery environment of the cell may cause HBTC to lose its capability of viscosity response. Therefore, HBTC needs to be further optimized.

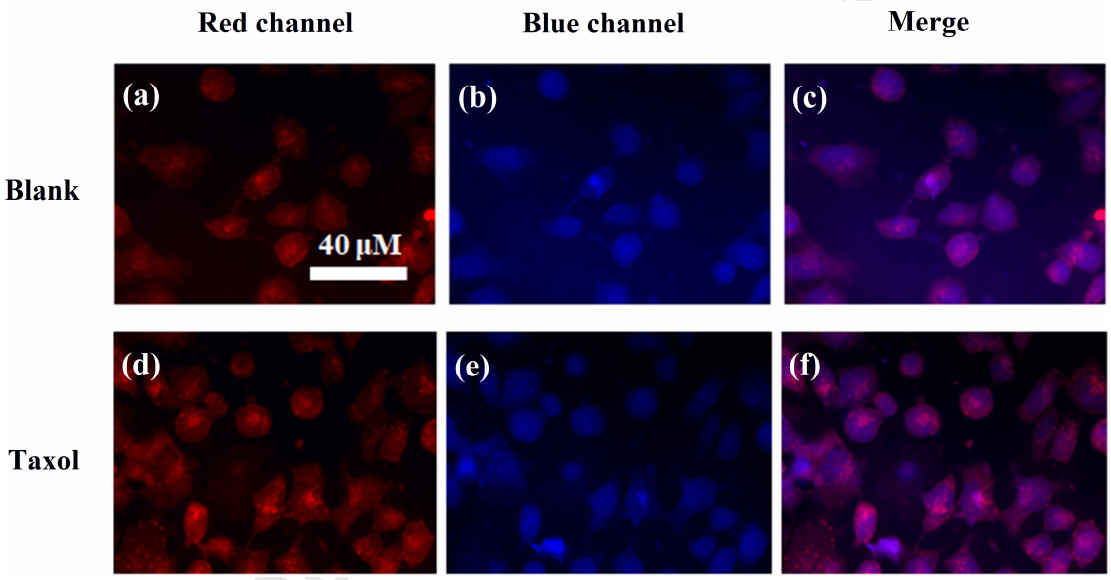

Fig. 5. Intracellular viscosity changes imaging by HBTC. (a) – (c) Photos of HBTC cultured cells in red channel, blue channel, and after merge; (d) – (f) Photos of Taxol (100 μg/ml) cultured cells in red channel, blue channel, and after merge.

Another function of HBTC is selective fluorescence response to OCl^-. In order to show the application of HBTC in response to OCl^- in cells, exogenous OCl^- was used as a stimulant to treat breast cancer cells cultured in HBTC. As shown in Fig. 6, HBTC mainly showed red fluorescence under blank conditions. After adding OCl^-, the fluorescence in the green channel was significantly enhanced and the fluorescence after Merge changed from red to yellow-green, which indicates that HBTC is responded by OCl^- with a ratiometric fluorescence signal.

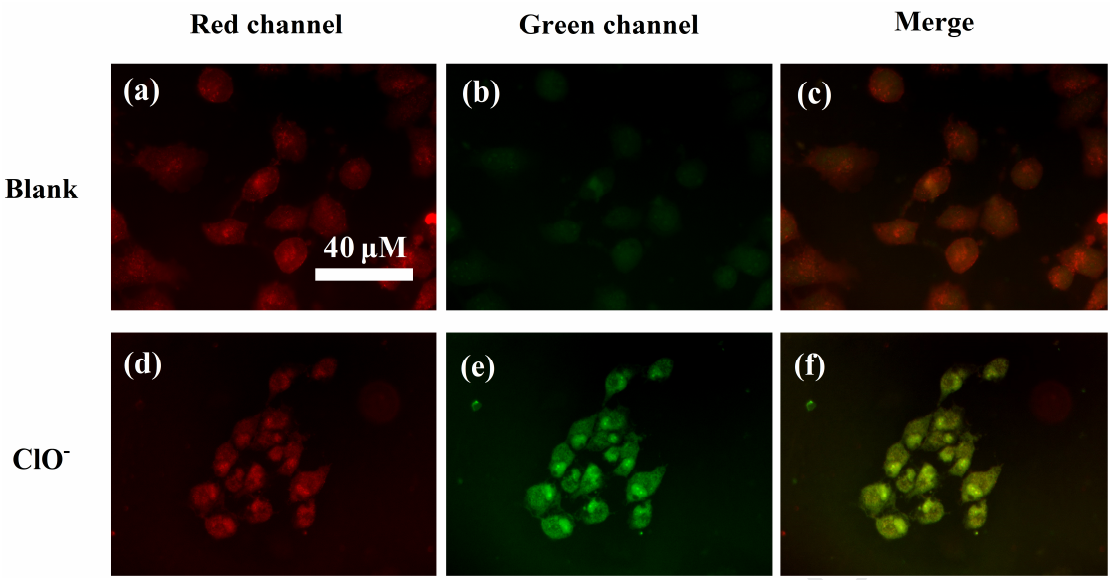

Fig. 6. OCl^- intracellular imaging by HBTC. (a) – (c) Photos of HBTC cultured cells in red channel, green channel, and after merge; (d) – (f) Photos of OCl^- treated cells in red channel, blue channel, and after merge.

Conclusion

In this work, a red-emitting fluorescent probe with 216 nm Stokes shift was synthesized for detecting viscosity and OCl^-. In the dissolved state, probe HBTC shows weak fluorescence, and the fluorescent intensity increases with the increase of environmental viscosity or the increase of water content, which shows the AIE property caused by the restriction of intramolecular rotation (RIR) effect. On the other hand, HBTC can selectively detect OCl^- by red-to-turquoise fluorescence signal with a LOD of 0.141 μM. At pH 6 – 9, HBTC was able to complete the detection in about 2 min. Finally, we apply the bifunctional probe HBTC to cell imaging. Viscosity changes caused by apoptosis did not result in significant fluorescence enhancement, but exogenous OCl^- causes a significant ratiometric fluorescence signal.

Acknowledgement

The work was supported by the National Natural Science Foundation of China (51678409, 51638011, 51578375, 81801808), Tianjin Research Program of Application Foundation and Advanced Technology (19JCYBJC19800, 18JCYBJC87500, 15ZCZDSF00880), State Key Laboratory of Separation Membranes and Membrane Processes (Z1-201507), Harbin Medical University Cancer Hospital Haiyan Foundation (JJZD2018-02), the Program for Innovative

Research Team in University of Tianjin (TD13-5042).

Reference

[1] Shen S-L, Zhao X, Zhang X-F, Liu X-L, Wang H, Dai Y-Y, et al. A mitochondria-targeted ratiometric fluorescent probe for hypochlorite and its applications in bioimaging. J. Mater. Chem. B. 2017;5(2):289-95.

[2] Lv J, Wang F, Wei T, Chen X. Highly Sensitive and Selective Fluorescent Probes for the Detection of HOCl/OCl^- Based on Fluorescein Derivatives. Ind. Eng. Chem. Res.. 2017;56(13):3757-64.

[3] Zhu B, Wu L, Zhang M, Wang Y, Liu C, Wang Z, et al. A highly specific and ultrasensitive near-infrared fluorescent probe for imaging basal hypochlorite in the mitochondria of living cells. Biosensors Bioelectron.. 2018;107:218-23.

[4] Jiang Y, Zhang S, Wang B, Qian T, Jin C, Wu S, et al. Novel triphenylamine-based fluorescent probe for specific detection and bioimaging of OCl^-. Tetrahedron. 2018;74(39):5733-8.

[5] Wu D, Chen L, Xu Q, Chen X, Yoon J. Design Principles, Sensing Mechanisms, and Applications of Highly Specific Fluorescent Probes for HOCl/OCl^-. Accounts Chem. Res.. 2019;52(8):2158-68.

[6] Zhu B, Wu L, Zhang M, Wang Y, Zhao Z, Wang Z, et al. A fast-response, highly specific fluorescent probe for the detection of picomolar hypochlorous acid and its bioimaging applications. Sensor. Actuat. B-Chem.. 2018;263:103-8.

[7] Nguyen KH, Hao Y, Zeng K, Fan S, Li F, Yuan S, et al. A benzothiazole-based fluorescent probe for hypochlorous acid detection and imaging in living cells. Spectrochim. Acta Part A. 2018;199:189-93.

[8] Jiang Y, Wu S, Jin C, Wang B, Shen J. Novel diaminomaleonitrile-based fluorescent probe for ratiometric detection and bioimaging of hypochlorite. Sensor. Actuat. B-Chem.. 2018;265:365-70.

[9] Pak YL, Park SJ, Xu Q, Kim HM, Yoon J. Ratiometric Two-Photon Fluorescent Probe for Detecting and Imaging Hypochlorite. Anal. Chem.. 2018;90(15):9510-4.

[10] Chen T, Chen Z, Liu R, Zheng S. A NIR fluorescent probe for detection of viscosity and lysosome imaging in live cells. Org. Biomol. Chem.. 2019;17(26):6398-403.

[11] Zhang Y, Li Z, Hu W, Liu Z. A Mitochondrial-Targeting Near-Infrared Fluorescent Probe for Visualizing and Monitoring Viscosity in Live Cells and Tissues. Anal. Chem.. 2019;91(15):10302-9.

[12] Chen B, Li C, Zhang J, Kan J, Jiang T, Zhou J, et al. Sensing and imaging of mitochondrial viscosity in living cells using a red fluorescent probe with a long lifetime. Chem. Commun.. 2019;55(51):7410-3.

[13] Gupta N, Reja SI, Bhalla V, Gupta M, Kaur G, Kumar M. A bodipy based fluorescent probe for evaluating and identifying cancer, normal and apoptotic C6 cells on the basis of changes in intracellular viscosity. J. Mater. Chem. B. 2016;4(11):1968-77.

[14] Yan Y-H, Ma H-L, Miao J-Y, Zhao B-X, Lin Z-M. A ratiometric fluorescence probe based on a novel recognition mechanism for monitoring endogenous hypochlorite in living cells. Anal. Chim. Acta. 2019;1064:87-93.

[15] Ye X, Xiang Y, Wang Q, Li Z, Liu Z. A Red Emissive Two-Photon Fluorescence Probe Based on Carbon Dots for Intracellular pH Detection. Small. 2019;15(48):1901673.

[16] Ma J, Si T, Yan C, Li Y, Li Q, Lu X, et al. Near-Infrared Fluorescence Probe for Evaluating Acetylcholinesterase Activity in PC12 Cells and In Situ Tracing AChE Distribution in Zebrafish. ACS Sensors. 2020;5(1):83-92.

[17] Yan Y-H, Wu Q-R, Che Q-L, Ding M-M, Xu M, Miao J-Y, et al. A mitochondria-targeted

fluorescence probe for the detection of endogenous SO2 derivatives in living cells. Analyst. 2020.

[18] Zhang N, He Y, Tang Q, Wang Y, Zheng Q, Hu P. A mitochondrial targeting two-channel responsive fluorescence probe for imaging the superoxide radical anion in vitro and in vivo. Talanta. 2019;194:79-85.

[19] Tang Y, Li Y, Lu X, Hu X, Zhao H, Hu W, et al. Bio-Erasable Intermolecular Donor–Acceptor Interaction of Organic Semiconducting Nanoprobes for Activatable NIR-II Fluorescence Imaging. Adv. Funct. Mate.. 2019;29(10):1807376.

[20] Zeng X, Xie L, Chen D, Li S, Nong J, Wang B, et al. A bright NIR-II fluorescent probe for breast carcinoma imaging and image-guided surgery. Chem. Commun.. 2019;55(95):14287-90.

[21] Tang Y, Pei F, Lu X, Fan Q, Huang W. Recent Advances on Activatable NIR-II Fluorescence Probes for Biomedical Imaging. Adv. Opt. Mater.. 2019;7(21):1900917.

[22] Zhou Z, Li Y, Su W, Gu B, Xu H, Wu C, et al. A dual-signal colorimetric and near-infrared fluorescence probe for the detection of exogenous and endogenous hydrogen peroxide in living cells. Sensor. Actuat. B-Chem.. 2019;280:120-8.

[23] Xu X, Chen W, Yang M, Liu X-J, Wang F, Yu R-Q, et al. Mitochondrial-targeted near-infrared fluorescence probe for selective detection of fluoride ions in living cells. Talanta. 2019;204:655-62.

[24] Si G, Zhou S, Xu G, Wang J, Wu B, Zhou S. A curcumin-based NIR fluorescence probe for detection of amyloid-beta (Aβ) plaques in Alzheimer's disease. Dyes Pigments. 2019;163:509-15.

[25] Zhao X-j, Jiang Y-r, Chen Y-x, Yang B-q, Li Y-t, Liu Z-h, et al. A new “off-on” NIR fluorescence probe for determination and bio-imaging of mitochondrial hypochlorite in living cells and zebrafish. Spectrochim. Acta Part A. 2019;219:509-16.

[26] Feng S, Liu D, Feng G. A dual-channel probe with green and near-infrared fluorescence changes for in vitro and in vivo detection of peroxynitrite. Anal. Chim. Acta. 2019;1054:137-44.

[27] Yan F, Bai Z, Zu F, Zhang Y, Sun X, Ma T, et al. Yellow-emissive carbon dots with a large Stokes shift are viable fluorescent probes for detection and cellular imaging of silver ions and glutathione. Microchim. Acta. 2019;186(2):113.

[28] Yang J, Fan M, Sun Y, Zhang M, Xue Y, Zhang D, et al. A near-infrared fluorescent probe based on phosphorus-substituted rhodamine for deep imaging of endogenous hypochlorous acid in vivo. Sensor. Actuat. B-Chem.. 2020;307:127652.

[29] Wang M, Chen N. Three-dimensional cellular imaging in thick biological tissue with confocal detection of one-photon fluorescence in the near-infrared II window. J. Biophotonics. 2019;12(7):e201800459.

[30] Qiu J, Jiang S, Lin B, Guo H, Yang F. An unusual AIE fluorescent sensor for sequentially detecting Co2+-Hg2+-Cu2+ based on diphenylacrylonitrile Schiff-base derivative. Dyes Pigments. 2019;170:107590.

[31] Yue Y, Huo F, Ning P, Zhang Y, Chao J, Meng X, et al. Dual-Site Fluorescent Probe for Visualizing the Metabolism of Cys in Living Cells. J. Am. Chem. Soc.. 2017;139(8):3181-5.

[32] Li H, Shi W, Li X, Hu Y, Fang Y, Ma H. Ferroptosis Accompanied by •OH Generation and Cytoplasmic Viscosity Increase Revealed via Dual-Functional Fluorescence Probe. J. Am. Chem. Soc.. 2019;141(45):18301-7.

[33] Wang J, Liu X, Pang Y. A benzothiazole-based sensor for pyrophosphate (PPi) and ATP: mechanistic insight for anion-induced ESIPT turn-on. J. Mater. Chem. B. 2014;2(38):6634-8.

[34] Liu H-W, Zhu X, Zhang J, Zhang X-B, Tan W. A red emitting two-photon fluorescent probe for dynamic imaging of redox balance meditated by a superoxide anion and GSH in living cells and

tissues. Analyst. 2016;141(20):5893-9.

[35] Ma Z, Sun W, Chen L, Li J, Liu Z, Bai H, et al. A novel hydrazino-substituted naphthalimide-based fluorogenic probe for tert-butoxy radicals. Chem. Commun.. 2013;49(56):6295-7.

[36] Khopkar S, Jachak M, Shankarling G. Novel semisquaraines based on 2, 3, 3, 8-tetramethyl-3H-pyrrolo [2, 3- f] quinoline: Synthesis, photophysical properties, AIE, viscosity sensitivity and DFT study. Dyes Pigments. 2019;161:1-15.

[37] Kumbhar HS, Deshpande SS, Shankarling GS. Aggregation induced emission (AIE) active carbazole styryl fluorescent molecular rotor as viscosity sensor. ChemistrySelect. 2016;1(9):2058-64.

[38] Dou Y, Kenry, Liu J, Zhang F, Cai C, Zhu Q. 2-Styrylquinoline-based two-photon AIEgens for dual monitoring of pH and viscosity in living cells. J. Mater. Chem. B. 2019;7(48):7771-5.

[39] Dong J, Pan Y, Wang H, Yang K, Liu L, Qiao Z, et al. Self-Assembly of Highly Stable Zirconium(IV) Coordination Cages with Aggregation Induced Emission Molecular Rotors for Live-Cell Imaging. Angew. Chem. Int. Ed.. 2019. https://doi.org/10.1002/anie.201915199.

[40] Sun Z-N, Liu F-Q, Chen Y, Tam PKH, Yang D. A Highly Specific BODIPY-Based Fluorescent Probe for the Detection of Hypochlorous Acid. Org. Lett.. 2008;10(11):2171-4.

[41] Yin W, Zhu H, Wang R. A sensitive and selective fluorescence probe based fluorescein for detection of hypochlorous acid and its application for biological imaging. Dyes Pigments. 2014;107:127-32.

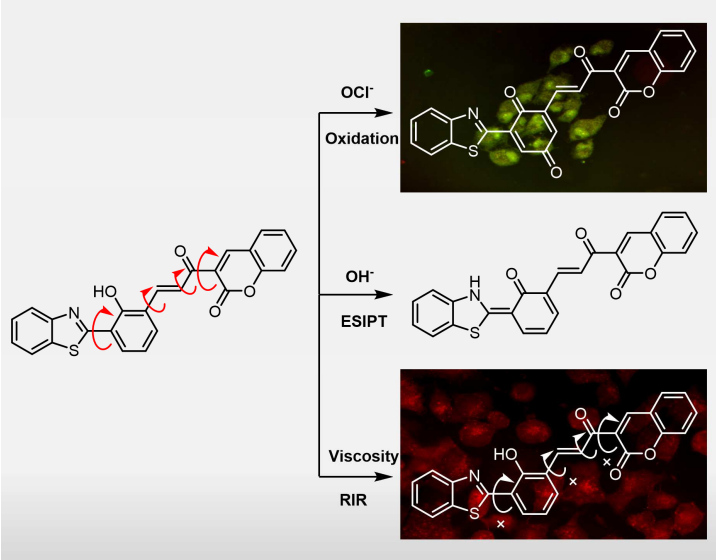

Graphic Abstract: HBTC fluorescence changes and cell imaging in three cases.

Highlight

1. A red-light emitting probe **HBTC** with 214 nm Stokes shift was synthesized.
2. Probe **HBTC** has dual functions response for viscosity and OCl^-.
3. Probe **HBTC** was successfully applied to the detection of OCl^- in MDA-MB-231 cells.

Conflict of interest

The authors declared that they have no conflicts of interest to this work.

We declare that we do not have any commercial or associative interest that represents a conflict of interest in connection with the work submitted